



## Measurement of U diffusion in Nb using $\alpha$ -Spectrometry

Perez Rodolfo A<sup>1-3\*</sup>, Gordillo Jorge A<sup>1</sup>, Iribarren M<sup>1,3</sup> and Di Lalla N<sup>2</sup>

<sup>1</sup>Gerencia de Materiales, Comisión Nacional de Energía Atómica (CNEA), de Buenos Aires, Argentina

<sup>2</sup>Consejo Nacional de Investigaciones Científicas y Técnicas- CONICET Avda. Rivadavia, Argentina

<sup>3</sup>Instituto Sabato-UNSAM/CNEA, San Martín, Argentina

\*Corresponding author: Rodolfo Ariel Perez, Avenida General Paz 1499, (B1650KNA) San Martín, Pcia. de Buenos Aires, Argentina, Tel: 0054-011-6772-7749; Fax: 0054-011-6772-7362; E-mail: rodperetz@cnea.gov.ar

Rec date: Jul 12, 2016 Acc date: Aug 19, 2016 Pub date: Aug 24, 2016

### Abstract

U bulk diffusion in Nb was measured by mean  $\alpha$ -spectrometry in the temperature range 1533 to 1673 K (1260 to 1400°C). Measurements obey the Arrhenius law with diffusion parameters  $Q = 423 \pm 10$  KJ/mol and  $D_0 = (2.5 \pm 1) \times 10^{-4}$  m<sup>2</sup>/s very close to the Nb self-diffusion ones found in the literature.

This behaviour is compatible with the hypothesis that U diffuses in the Nb lattice via a vacancy mechanism, at the same time it is in disagreement with previous measurements of U diffusion performed at higher temperatures, where the activation energy is significant lower.

**Keywords:** Diffusion; Metals; Energy materials;  $\alpha$ -spectrometry

### Introduction

The present work is part of a larger and systematic investigation on U diffusion at infinite dilution in metals with particular emphasis on those used in the nuclear industry.

The interest on the subject lies in the fact that the available U diffusion coefficients at infinite dilution in the literature are scarce, mostly measured in the 60's and 70's Cf Ref. [1] for a list of the measurements performed up to 1990, with values somehow controversial. Besides, a quick (probably not exhaustive) literature search (e.g. Ref. [2] and the Scopus data base) suggests there are no measurements of diffusion at infinite dilution in pure metals newer than the mentioned ones.

Regarding U diffusion in Nb at infinity dilution there are two previous measurements; both follow the Arrhenius law:

$$D(T) = D_0 \exp\left(-\frac{Q}{RT}\right) \quad (1)$$

Where, D is the diffusion coefficient at a given temperature T (in K) Q is activation energy, D<sub>0</sub> is so called pre-exponential factor and R is the gas constant 8.31451 J/(mol-K)

In the first one [3] the integral residual activity method (Gruzin) was applied to 99.55% purity polycrystalline samples in [1773-2273 K]

temperature range with diffusion parameters  $Q = 321.5$  kJ/mol-K and  $D_0 = 8.9 \times 10^{-6}$  m<sup>2</sup>s<sup>-1</sup>.

The second one [4], measured in the range [1993-2373 K], reports  $Q = 321.1$  kJ/mol-K, a value similar to the first work, but a  $D_0 = 5.0 \times 10^{-10}$  m<sup>2</sup>s<sup>-1</sup>, which implies that, in the superposed temperature ranges between both measurements, the differences between D values are around four order of magnitude.

On the other hand, Nb self-diffusion was carefully measured by several authors (see [5] and references therein) in single crystal and polycrystalline samples covering ten orders of magnitude in D, in an extended temperature range 1150 to 2670 K; considering all the works together, in such extended range a slight curvature in the Arrhenius plot is observed. Neumann et al. in [5] analyze several different ways to fit the experimental data in order to get the temperature dependence of D, considering essentially two possible mechanisms responsible for the curvature: (a) two different defects, mono and divacancies, mediating the diffusion process, or (b) a temperature dependence of energies and entropies of vacancy formation and migration. We are going to review this subject in order to compare our measurements with the self-diffusion in the discussion section.

Given the ability of the  $\alpha$ -spectrometry technique [6] to measure submicrometric diffusion profiles, in the present work diffusion coefficients for U in Nb were obtained in a lower temperature range than the ones in [3,4], below  $2/3 T_m$ , being  $T_m$  the Nb melting temperature (2742 K), where the influence of divacancies in the diffusion process is, presumably, negligible.

### Materials and Methods

The measurements were performed in high purity (99.9 %) discs of Nb of 20 mm in diameter and around 3 mm thickness. Table 1 reports a complete list of the impurity content. Polycrystalline samples were used with a grain size of several mm; a micrography of a typical sample is shown in Figure 1.



**Figure 1:** Optical micrography (5x) corresponding to a typical Nb sample.

Element	Content ( $\mu\text{g/g}$ )
Al	<10
B	2
Ca	<10
Co	<10
Cr	<10
Cu	<10
Fe	<10
Mg	<10
Mn	<10
Mo	<10
Ni	<10
Si	<10
Sn	<10
Ta	255
Ti	20
W	<100
Zr	<10
C	25
H	<10
O	230
N	35

**Table 1:** Nb samples impurity contents.

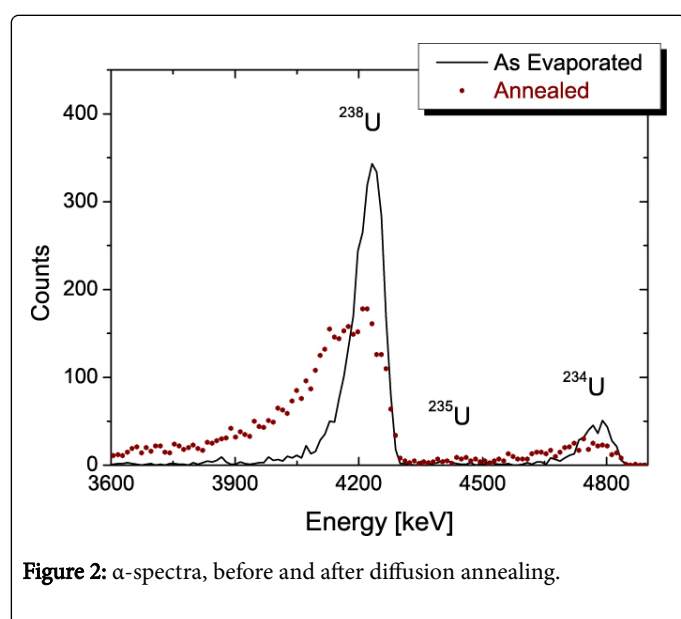


**Figure 2:**  $\alpha$ -spectra, before and after diffusion annealing.

The samples were mechanically polished and chemically polished, then subjected to an annealing of 24 hs at 1673 K in vacuum in order to relieve stress.

Diffusion pairs were obtained by evaporation of depleted U, 99.97% purity, onto the sample surface, by heating a tungsten filament in a vacuum better than  $10^{-6}$  torr. The  $\alpha$ -spectrum taken after the deposition and before diffusion annealing (Figure 2) shows, through the analysis presented in section 3, that the U layer deposited is less than 9 nm.

The diffusion anneals were performed under dynamic vacuum,  $2 \times 10^{-6}$  torr in ceramic tubes. To prevent reactions between Nb and mullite samples were wrapped into Ta foils. The diffusion temperatures were controlled within  $\pm 1$  K with a Pt-PtRh S type thermocouple. Correction for hit up times were performed.

A silicon base p-n junction surface barrier detector (Canberra PD 150-16-100-AM) was used in order to measure the  $\alpha$ -spectra, with an active surface of  $150 \text{ mm}^2$  and an energy nominal resolution of 16 keV. As neither the detector nor the samples are points, the solid angle subtended between them is not unique. In order to test their influence in the peak width we change the sample-detector distance between 2 and 10 cm, inside the vacuum chamber. Of course, an increment in the distance implies an increment in the acquisition time, but not significant variation in the peak width was observed. Consequently, in order to minimize the acquisition time, a distance of 2 cm between sample and detector was chosen. Typical acquisition times were between 20 and 40 h.

Calibration in energy was made using three  $\alpha$  peaks from a  $^{241}\text{Am}$  standard source, one from a  $^{233}\text{U}$  standard source and the last one is the  $^{238}\text{U}$  peak, so energy (E) as function of channel number (ch) is given by  $E(\text{ch}) = (175.31 + 11.39 \times \text{ch}) \text{ keV}$ .

The (as evaporated) initial spectra was fitted with a gaussian function whose width is given by the convolution of the effect of the  $\alpha$ -emission depth across the U deposit, the electronic noise, and the difference in the particle path due to the solid angle subtended between the sample and the active surface of the detector. Other noise contributions, like straggling, could be neglected. In this particular case, the initial width was 45 keV.

## Data Analysis

The spectra of  $\alpha$ -particles emitted by U at different depth in the material, after the diffusion annealing, is converted into diffusion profiles combining the knowledge on the stopping power of  $\alpha$ -particles coming from particles accelerators into an algorithm developed in [6], where a full description of the method in a general case is given. In what follows the application to the specific case of U diffusion in Nb is described.

The  $\alpha$ -particles spectra measured after U deposition and before the diffusion annealing is shown as full line in Figure 2; the analysis is focused in the particles emitted by the  $^{238}\text{U}$  isotope. After annealing, there is a spectrum broadening towards low energies plotted in the same Figure 2 as dotted line. The broadening is given by the increase in the emitter distance to the surface due to diffusion, entailing larger energy losses.

The stopping power ( $dE/dx$ ) as defined, for instance, in ref [7] represents the amount of energy loss by the  $\alpha$ -particle during the path between the point of emission and the surface. The stopping power was

calculated with the subroutine “stopping range” from the program SRIM 2008 [8] for  $\alpha$ -particle moving in Nb between 10 keV and 5 MeV, with an error estimation lower than 3%.

The  $\alpha$ -particle stopping power dependence with the energy in solid Nb is plotted in Figure 3. The solid line is a parabolic fit of the data valid between 800 keV and 5 MeV:

$$dE/dx(E) = a + b \cdot E + c \cdot E^2 \quad (2)$$

Being  $a = 87.295855 \text{ eV } \text{\AA}^{-1}$ ,  $b = -1.9831912 \cdot 10^{-5} \text{ \AA}^{-1}$  and  $c = 1.803833 \cdot 10^{-12} \text{ eV}^{-1} \text{ \AA}^{-1}$ .

Then, when the  $\alpha$ -particle is emitted by a  $^{238}\text{U}$  atom from a distance  $x$  to the surface,  $x$  can be obtained from the integration of the stopping power over the whole path:

$$x = - \int_{E_0}^{E_d} \frac{dE}{dE/dx} = - \int_{E_0}^{E_d} \frac{dE}{a + bE + cE^2} \quad (3)$$

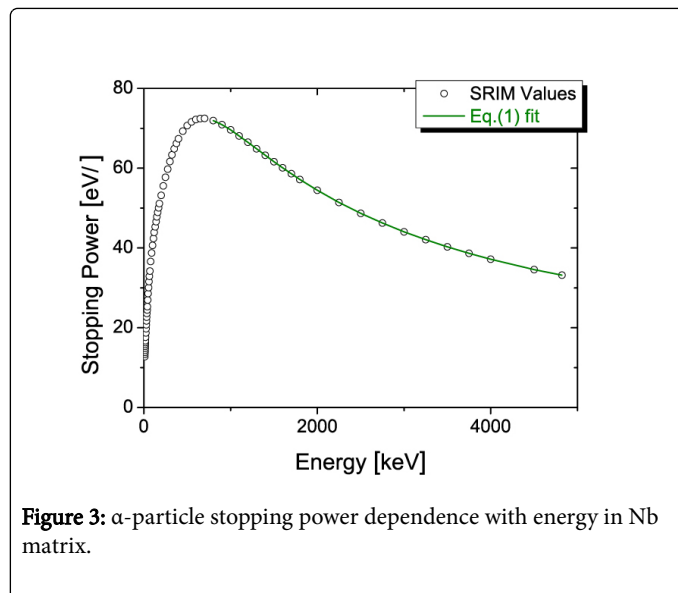


**Figure 3:**  $\alpha$ -particle stopping power dependence with energy in Nb matrix.

Where,  $E_0$  is the energy of the  $\alpha$ -particle when emitted (4.267 MeV) and  $E_d$  is the detected energy when arriving at the sample surface.

Analytic integration of expression (3) is straightforward, giving a relationship between the U depth and the detected energy:

$$x(E_d) = \frac{1}{\sqrt{ac - (b/2)^2}} \left[ \arctan\left(\frac{cE_0 + b/2}{\sqrt{ac - (b/2)^2}}\right) - \arctan\left(\frac{cE_d + b/2}{\sqrt{ac - (b/2)^2}}\right) \right] \quad (4)$$

When  $(b^2 - 4ac) < 0$ , as in the present case.

Throughout Equation (4) a direct relationship between energy lost and depth, and consequently, with the spectrum channel number can be obtained.

The amount of U at each depth is directly related to the amount of counts cumulated in that channel, given in arbitrary units.

The information in order to obtain a typical diffusion profile, U concentration versus depth, is now available from the (Number of Counts) versus (Channel Number)  $\alpha$  spectra profiles.

## Results and Discussion

The Gaussian solution to Fick's law is used to fit the profiles since the initial thickness of the U deposited is thicker than the diffusion path and the U solubility in the Nb matrix is large enough:

$$C(x) = \frac{C_0}{\sqrt{\pi D(t + t_0)}} \exp\left(-\frac{x^2}{4D(t + t_0)}\right) \quad (5)$$

Where,  $C$  is the U concentration at depth  $x$ ,  $C_0$  is the initial amount of U per unit of area at the surface,  $D$  is the diffusion coefficient at a given temperature,  $t$  is the annealing time and  $t_0$  is a fitting parameter coming from the initial profile (before the diffusion annealing) used in order to perform a deconvolution to its initial width as described in [6].

All the diffusion profiles  $\ln[C(x)]$  versus  $x^2$  were built with the algorithm described in the previous section 3. They are shown, for each temperature studied, in Figure 4. In all cases Equation (5) is satisfied since straight lines were obtained; that means all the deposited U diffuses in solid solution in the Nb matrix. Diffusion coefficients were obtained from:

$$D = \frac{s - s_0}{4ts_0} \quad (6)$$

Where,  $s$  is the slope of the diffusion profile and  $s_0$  is the one of the as-evaporated initial profile.

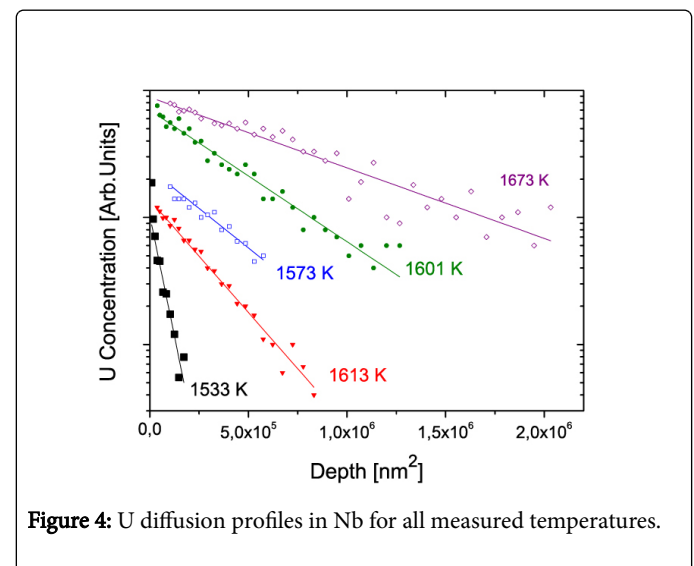


**Figure 4:** U diffusion profiles in Nb for all measured temperatures.

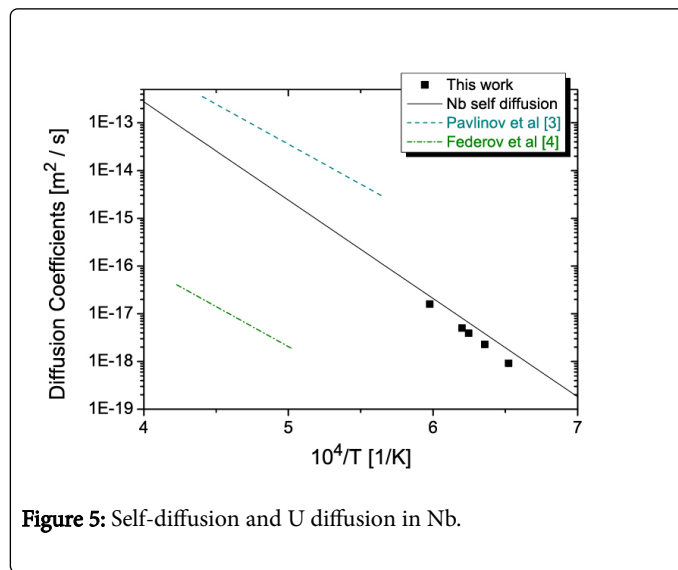
A complete list of temperatures, diffusion annealing times and  $D$  values at each temperature is given in Table 2.

Figure 5 is an Arrhenius plot [ $\ln(D)$  vs  $T^{-1}$ ] for all those  $D$  values. In the temperature range measured a straight line fit all diffusion coefficients quit well with the following parameters:

$$D(T) = (2.5 \pm 1.0) \cdot 10^{-4} \exp\left(\frac{-(423 \pm 10 \text{ kJ/mol})}{kT}\right) \text{ m}^2 \text{ s}^{-1} \quad (7)$$

Temperature	Effective annealing time [s]	D[m <sup>2</sup> s <sup>-1</sup> ]
1673	11.640	(1,5 ±0,5) × 10 <sup>-17</sup>
1613	11.580	(5,0 ±0,7) × 10 <sup>-18</sup>
1601	25.740	(3,9 ±0,3) × 10 <sup>-19</sup>
1573	11.540	(2,3 ±0,2) × 10 <sup>-18</sup>
1533	11.510	(9.2 ±4.0) × 10 <sup>-19</sup>

**Table 2:** D values measured at different temperatures.



**Figure 5:** Self-diffusion and U diffusion in Nb.

Also in Figure 5 Nb self-diffusion is shown for comparison. As we pointed out in the introduction, the self-diffusion was measured by several authors [5] in an extended temperature range, covering ten orders of magnitude in D. All the available data for self-diffusion was analyzed by Neumann [5] in different ways.

On one hand, the assumption that two different defects or at least two different jump types are responsible for the soft curvature of the Arrhenius plot was made. When divacancy, self-interstitial and/or next-nearest neighbour monovacancy jumps in the high-temperature range could be considered as a second mechanism becoming dominant in the diffusion flux, the temperature dependence of D is given by:

$$D(T) = D_0^1 \exp\left(\frac{Q_1}{kT}\right) + D_0^2 \exp\left(\frac{Q_2}{kT}\right) \quad (8)$$

Where,  $D_0^1$  and  $Q_1$  are the diffusion parameters for monovacancies and  $D_0^2$  and  $Q_2$  for the second mechanism; assumed as divacancies in the Nb self-diffusion case.

Fitting parameters, obtained by Neumann considering different sets of data and/or different mathematic algorithms are, for monovacancies:  $D_0^1$  between  $1.3 \times 10^{-5}$  and  $5.4 \times 10^{-6}$  m<sup>2</sup>s<sup>-1</sup>,  $Q_1$  between 360 and 400 kJ/mol. For divacancies:  $D_0^2$  between  $3.54 \times 10^{-2}$  and  $1.18 \times 10^{-3}$  m<sup>2</sup>s<sup>-1</sup>, and  $Q_2$  between 470 and 540 kJ/mol.

On the other hand, Köhler and Herzog [9] in a careful study in the  $\beta$ -phase of the group IVb metals ( $\beta$ -Ti and  $\beta$ -Zr), minimize the influence of divacancies and postulate that the enhanced diffusivity can be explained by the softening of the longitudinal acoustic (LA)<sub>2/3</sub>

<111> phonon mode. So, for all these metals the entire curvature of ln D against 1/T arises from the temperature dependence of the vacancy migration energy. Moreover, they suggest that the diffusion behaviour in all b.c.c. metals can be described in terms of the phonon mode softening as an intrinsic characteristic of these structures that diminishes the energy required to move a vacancy when the temperature goes down; in the particular case of IVb metals, when the temperature reaches  $T_{\alpha/\beta}$  occurs the phase transition.

When Neumann [5] considered the curvature of the Arrhenius plot as the result of energies and entropies temperature dependence for vacancy formation and migration,  $D(T)$  is described by [10]

$$D(T) = D_0^\alpha \exp\left(-\frac{Q^\alpha}{kT}\right) \exp\left[2\alpha \ln\left(\frac{T}{T_0}\right) - 2\alpha \frac{(T - T_0)}{T}\right] \quad (9)$$

Which is based on the assumption of linear temperature dependences of the vacancy formation energy  $H^F$  and migration energy  $H^M$ , that is  $H(T) = H(T_0) + \alpha k(T - T_0)$ , with  $Q = H^F + H^M$  and  $2\alpha = \alpha^F + \alpha^M$ .  $T_0$  is a reference temperature larger than the Debye temperature; being  $\alpha$  in Equation (9) a good measure for the degree of the curvature of the Arrhenius plot. Neumann takes  $T_0 = 700$  K (around  $T_m/4$ ) and fit all the measured self-diffusion coefficients with:

$$D(T) = 4.1 \times 10^{-4} \exp\left(\frac{326 \text{ kJ/mol}}{kT}\right) \exp\left[7.4 \ln\left(\frac{T}{700}\right) - 7.4 \frac{(T - 700)}{T}\right] \quad (10)$$

There is practically no difference between the fitting applying Equation (8) or (10), so the full line in Figure 5 represents the Nb self-diffusion in any case.

The present work results shown also in Figure 5, are close to the self-diffusion ones but systematically lower by a factor between 0.5 and 0.7. Then, U can be considered as a substitutional diffuser in Nb, as expected given its mass and atomic radius.

Even when this behaviour could be interpreted as a simple mass effect (the mass of U is 2.6 times larger than the Nb one) the electronic structure of the diffusant used to be relevant and can invert this relationship (for example in the U diffusion in  $\alpha$ -Ti [11]); what remains is that, for substitutional diffusers, D values must not differ in plus/minus one order of magnitude than self-diffusion.

Given the shorter temperature range measured in this work, not curvature in the Arrhenius plot is observable. Since this range is below  $2/3 T_m$  influence of divacancies are not expected, and since it is also above one third of  $T_m$  the effect of phonon softening should not be noticeable, a straight Arrhenius plot for U diffusion, as shown in Figure 5, is reasonable. Also, diffusion parameters Q and  $D_0$  are compatible with a vacancy mechanism being dominant in the measured temperature range.

When we compare the present results with the previous measurements of U diffusion in Nb [3,4], the first thing to notice is the low values of activation energies for both measurements ( $Q = 321.1$  and  $321.5$  kJ/mol respectively) if we take into account that vacancy energy formation in Nb are between 290 and 350 kJ/mol according to experimental measurements [12,13].

Measurements in [3] were performed in polycrystalline samples of 99.55 % purity using the residual activity technique in a higher temperature range 1773 to 2273 K. D values are more than one order of magnitude higher than the self-diffusion ones. Extrapolation of

those values to the lower temperature measured in this work increases the differences up to more than two orders of magnitude. Even when the grain size of the samples was not reported in [3], it is very likely that their D values were convoluted with diffusion along short circuits.

In fact, being the depth of analysis for  $\alpha$ -spectrometry (from tenth to a few  $\mu\text{m}$ ) two orders of magnitude lower than for residual activity and given the grain size of our samples, shown in Figure 1, the contribution to the diffusion flux via grain boundaries in our measurements is negligible. The same differences were found for U diffusion in other metals under similar circumstances [11,14]

Differences with [4] are harder to understand. Measured in a similar temperature range 1993 to 2373 K than [3] in uncharacterized polycrystalline samples with an unreported experimental technique, D values are exactly 4 orders of magnitude lower than the measured in [3] and almost 3 orders of magnitude lower than self-diffusion. As we do not have access to the original Russian paper but to an English translation, we wonder if in the values also reported in compilation books [1] page 116 and [2] page 223, could have an origin in a mistake coming from the conversion of the old way to report D values in  $\text{cm}^2\text{s}^{-1}$  to the MKS in  $\text{m}^2\text{s}^{-1}$ , which is exactly 4 orders of magnitude.

## Conclusions

U diffusion in Nb in the temperature range 1533 to 1673 K was determined using  $\alpha$ -spectrometry. It follows the Arrhenius law with diffusion parameters Q and  $D_0$  close to the self-diffusion via mono-vacancies ones, which means a vacancy mechanism is dominant in the measured temperature range.

Comparison with previous works shows discrepancies probably due to the previous values are effective diffusion coefficients product of convolution between bulk and short circuits diffusion. The same differences were found for U diffusion in other metals under similar circumstances, since the use of  $\alpha$ -spectrometry in polycrystals with grain size larger than 100  $\mu\text{m}$  minimize the short circuits influence in the diffusion flux.

At the light of this results, we finally conclude that the results of U diffusion at infinite dilution obtained in early works need to be revised

and extended to lower temperature ranges using sub-micrometric techniques like the  $\alpha$ -spectrometry.

## References

1. Mehrer H (1990) Diffusion in solid metals and alloys. Landolt-Börnstein. Springer-Verlag Berlin Heidelberg.
2. Neumann G, Tujin C (2009) Self-diffusion and impurity diffusion in pure metals: Handbook of Experimental Data (1st edn). Pergamont Materials Series, Elsevier Ltd, Amsterdam, Netherlands.
3. Pavlinov LV, Nakomechnicov VN, Bykov VN (1965) Sov J Atomn Energiya, English Transl 19: 1495-1501.
4. Federov GB, Smirnov EA, Zhomov FI, Gusev FI, Paraev SA (1971) Sov J Atomn Energiya, English Transl 31: 1280-1286.
5. Neumann G, Tölle V (1990) Self-diffusion in body-centred cubic metals: Analysis of experimental data. Philos Mag A 61: 563-578.
6. Pérez RA, Gordillo JA, Di Lalla N (2012) Difusión de U EN Nb. Measurements 45: 1836-1841.
7. Chu WK (1986) Rutherford backscattering spectrometry. ASM Handbook Vol 10. Materials Characterization. ASM International, Member/Customer Service Center, Materials Park, OH 44073-0002, USA.
8. Ziegler JF, Biersack JP, Ziegler MD (2008) SRIM - The Stopping and Range of Ions in Matter.
9. Köhler U, Herzig Ch (1988): Philos. Mag. A 58: 769-781.
10. Seeger D, Mehrer H (1970) Vacancies and Interstitials in Metals. Amsterdam- North-Holland.
11. Pérez RA, Gordillo JA, Di Lalla N (2013) Philos Mag A 93: 2219-2228.
12. Faber K, Schweikhardt J, Schultz H (1974) The Intrinsic Stage-III Annealing in Niobium and Tantalum following Electron Irradiation. Scripta Metallurgica 8: 713-720.
13. Schuirlich IA, Shultz H (1980) Quenching experiments on niobium. Philos Mag A 42: 613-620.
14. Pérez RA, Gordillo JA, Di Lalla N, Iribarren M (2015) Journal of Nuclear Material 462: 85-90.